J Mater Sci: Mater Electron (2017) 28:18515–18528
DOI 10.1007/s10854-017-7799-0

CrossMark

The growth behavior of interfacial intermetallic compound between Sn–3.5Ag–0.5Cu solder and Cu substrate under different thermal-aged conditions

Tao Xu[1] · Xiaowu Hu[1] · Yulong Li[1] · Xiongxin Jiang[1]

Received: 23 June 2017 / Accepted: 28 August 2017 / Published online: 4 September 2017
© Springer Science+Business Media, LLC 2017

Abstract The interfacial reaction, morphology, activation energies and growth behavior of interfacial intermetallic compounds (IMCs) between the Sn–3Ag–0.5Cu (in wt%) solder and Cu substrate during reflow at 280 °C for 10 min and aging at different temperatures for up to 360 h were investigated, and the growth kinetics of the interfacial Cu–Sn binary IMC layers were monitored during the isothermal aging. The results showed that the thickness of IMCs increased linearly with square root of aging time, and the diffusion coefficient related to the Cu–Sn IMC layer increased with increasing aging temperature. During aging at medium temperature (180 °C), the scallop-like Cu_6Sn_5 IMC layer at the SAC305/Cu interface gradually transformed into planar type with prolonged aging time. Nevertheless, in the case of high temperature (200 °C) aging, the solder/Cu_6Sn_5 interface became uneven because the Cu atoms came from the bulk solder would accumulate on the Cu_6Sn_5 IMC surface to directly thicken the existed IMC layer. Beside, the Kirkendall voids within Cu_3Sn layer and the neighborhood of the Cu_3Sn/Cu interface almost aggregated into continuous regions to formed micro-voids. The activation energies of the total Cu–Sn, Cu_6Sn_5 and Cu_3Sn IMCs were obtained by plotting the diffusion constants (D) as a function of the aging temperature ($1/T$), and were 115.2, 122 and 98 kJ/mol, respectively.

✉ Xiaowu Hu
huxiaowu@ncu.edu.cn

[1] Key Lab for Robot and Welding Automation of Jiangxi Province, Mechanical and Electrical Engineering School, Nanchang University, Nanchang 330031, China

1 Introduction

The development of substitutional Pb-free solder has become important for electronic interconnection materials due to the toxicity of Pb which excessively threatens the human health and the environment [1–4]. Among the various alternative lead-free solders, SnAgCu-based (SAC) solders are one of most promising Pb-free solder alloys as low melting point, good wetting properties and good mechanical properties [5–7].

Generally speaking, Cu is widely used as the substrate materials in electronics packaging. The nucleation and growth of intermetallic compounds (IMC) during the soldering process are regarded as a key indication of a good metallurgical bond between solder alloys and Cu substrate. At the same time, the IMCs (Cu_6Sn_5 and Cu_3Sn) which come from reaction between SAC solder and Cu substrate will rapidly grow, and the kirkendall voids will form at the Cu_3Sn/Cu interface during reflowing and aging process. It is accepted that the IMC tends to concentrate stress and create defects under stress conditions [8–13]. The excessive growth of intermetallic compounds may undermine the reliability of solder joint because of the brittleness of the intermetallic compounds layer. Besides, the stress concentration come from the generation of kirkendall voids and consumption of the substrate also degrades the reliability of solder joint [9, 14–17]. It is, therefore, particularly critical to understand the growth mechanism of microstructure of solder joint. That will be helpful to find a way to inhibit the growth of IMCs and formation of voids or protect the substrate.

In the past decades, the interfacial reactions and IMC growth behaviors between Sn3Ag0.5Cu (SAC305) solder and Cu substrate have been studied by some researchers [8, 9, 16–18]. Yu et al. [19] introduced the intermetallic compounds growth between Sn–3.5Ag lead-free solder and Cu

substrate by dipping method. The samples aged at 170 °C for 1000 h were investigated. Liang Zhang et al. [20] pointed out the growth kinetics and activation energies of IMC layers between Sn3.8Ag0.7Cu and Cu substrate, which aging at temperature 100–140 °C. On the other hand, the solder volume and Cu concentration also have effect on the interfacial reaction. Such as, Yang et al. [7] studied the effects of Cu concentration in solder, solder volume and aging temperature (160 and 180 °C) on solid-state reaction. Although the growth mechanism and growth kinetics of Cu_6Sn_5 have been studied, the effects of bulk solder versus various aging temperature, especially at high aging temperature (200 °C), on the morphology and growth kinetics of the IMC formed between SAC305 and Cu substrate during solid-state aging are still lack. Therefore, it is necessary to fully understand the growth behavior and morphology of IMCs with bulk solder at different solid-state aging temperature process.

In this paper, we formed the IMC with a reflowing method by using a reflow furnace which is equipped with time control devices to maintain the soldering time. The grain morphology, activation energies and growth kinetics of IMCs formed between bulk SAC305 solder and Cu substrate under various aging temperature were studied. The different morphology of IMC at high aging temperature were studied. The ripening process and the growth mechanism of IMCs were discussed, too.

2 Experimental procedure

In this work, the commercial Sn3.0Ag0.5Cu (SAC305) solder paste was employed. Pure Cu plate (99.99%) with dimensions of $10 \times 10 \times 2$ mm^3 was used in this experiment served as the substrate. Before soldering, the cooper surface was carefully polished by using 0.1 µm diamond paste, and then rinsed in water and methanol alcohol. The equivalently solder paste (about 3 mm diameter) were placed on the fresh Cu pads, as shown in Fig. 1a. Then the reflow process was performed as following: first step, the prepared specimens were placed in an oven; second step, the oven was heated from room temperature to the preheating at 150 °C for 100 s, then reflowing at 280 °C for a constant time of 600 s; finally, the reflowed specimens were cooled in air. After soldering, the soldered samples were subjected to three different isothermal aging treatments (120, 180 and 200 °C) for 24, 120, 240 and 360 h in oven, respectively.

After isothermal aging, two samples derived from the single soldered sample by wire cutting were prepared to study each parameter by observing the cross-sectional structure (as shown Fig. 1b) and the top view (direction perpendicular to the interface) of the IMC morphology by using scanning electron microscope (SEM). One-half of sample was mounted in epoxy and polished to remove the skin layer to reveal the cross-sectional microstructure; the other half was immersed in corrosive liquid (20 vol% HNO_3 solution) with ultrasonic waves to dissolve away the excess solder and expose the three-dimensional IMC feature.

In order to get accurate thickness data of the IMCs, the thickness and microstructure of interfacial reaction region between solder and substrate were investigated by SEM (QUANTA 200F) at a voltage of 20 keV. Detailed morphologies of the IMC layer surface were revealed using secondary electron model.

The IMC equivalent thickness was measured using the SEM images of the metallographic cross-sections and the following image analysis procedure. (1) A SEM image of each sample was obtained at the appropriate magnification. (2) The grayscale SEM image was enhanced using image analysis software to clearly identify the interfaces between the different layers and their pixels. (3) The mean equivalent thickness (L_{IMC}) of the individual layer was calculated using the following equation:

$$L_{IMC} = (N_{IMC}/N_{SEM}) \times L_{SEM} \quad (1)$$

In which L_{SEM} is the actual height of the individual SEM image, and N_{IMC} and N_{SEM} are the number of pixels in the IMC layers and the entire SEM image, respectively. To improve the statistical reliability of the IMC layer-thickness data, at least 15 SEM images covering numerous grains in the middle of the interface were analyzed for each sample. The errors of each IMC equivalent thickness were obtained by using the standard deviation function from the measured data.

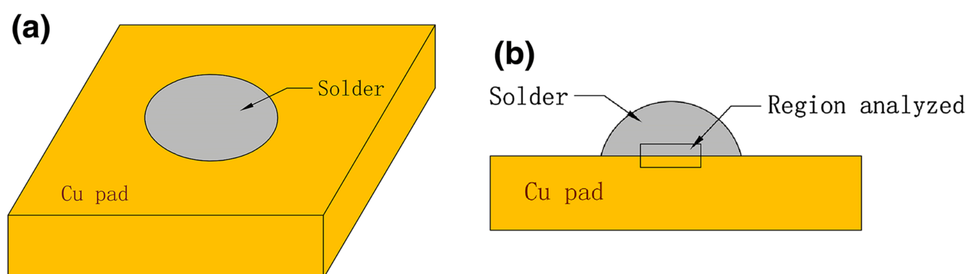

Fig. 1 Schematic diagram of solder joints, **a** soldered joint; **b** cross-section of the analyzed region

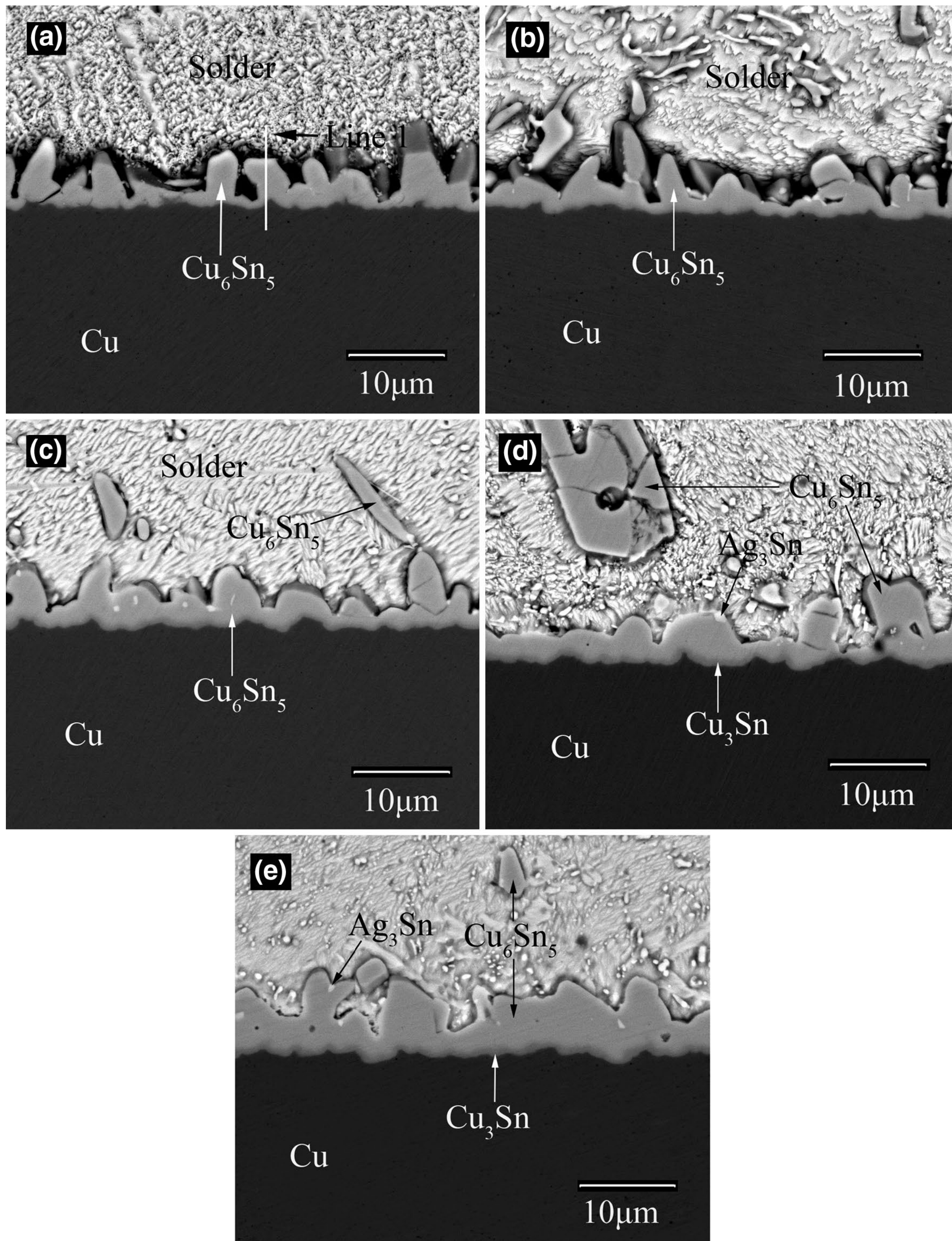

Fig. 2 Cross-sectional microstructure of SAC305/Cu interfaces reflowed at 280 °C for 10 min and aged at 120 °C for various time, **a** reflowed only; **b** 24 h; **c** 120 h; **d** 240 h; **e** 360 h

3 Results and discussion

3.1 Interfacial microstructure and EDS analysis of aged SAC305/Cu couples

Figure 2a–e show the BEI (back-scattered electron image) micrographs of IMC layer for the interface between Sn3.5Ag0.5Cu solder and Cu substrate after the liquid–solid reaction at 280 °C for 10 min and aged at 120 °C for various times. It is clearly seen that only one IMC layer was observed between solder and Cu substrate after reflowing and aging for 24 h as shown in Fig. 2a and b, respectively. The interfacial layer of Cu–Sn IMC was composed of two IMC phases in the prolonged aging samples, as shown in Fig. 2c–e, respectively. To identify the primary phases formed at the interface of samples, three typical compounds with different gray level were detected by using EDS (Energy dispersive X-ray spectroscopy). Figure 4a–c correspond to the EDS patterns of spectrums 1–3 in Fig. 3c, respectively. Figure 4a confirms that the white bulk embedded in the IMC layer is indeed Ag_3Sn compound, which is composed of 74.4 at.% Ag and 25.6 at.% Sn. Figure 4b reveals that the IMC layer adjacent to the bulk solder is Cu_6Sn_5 IMC, which is the thickest IMC layer between solder and Cu substrate, composed of 52.86 at.% Cu and 47.14 at.% Sn. Figure 4c shows that the IMC adjacent to Cu substrate is Cu_3Sn IMC which is composed of 73.94 at.% Cu and 26.06 at.% Sn. Besides, it was observed that the nubby Cu_6Sn_5 IMC dispersed at the middle of bulk solder, as shown in Fig. 2c, d.

In Fig. 2a, the sole IMC layer, which exhibited scallop-like appearance, composed of Cu_6Sn_5 phase was confirmed. To further figure out the situation of interface between solder and substrate, the elemental line scan was applied. The position of line scan 1 was marked by white line as shown in Fig. 2a and the results of elemental line scan were listed in Fig. 5. Figure 5a shows the close-up of the line scan 1 in Fig. 2a. Figure 5b shows the elemental counts of the line scan 1, which reveals that there are three

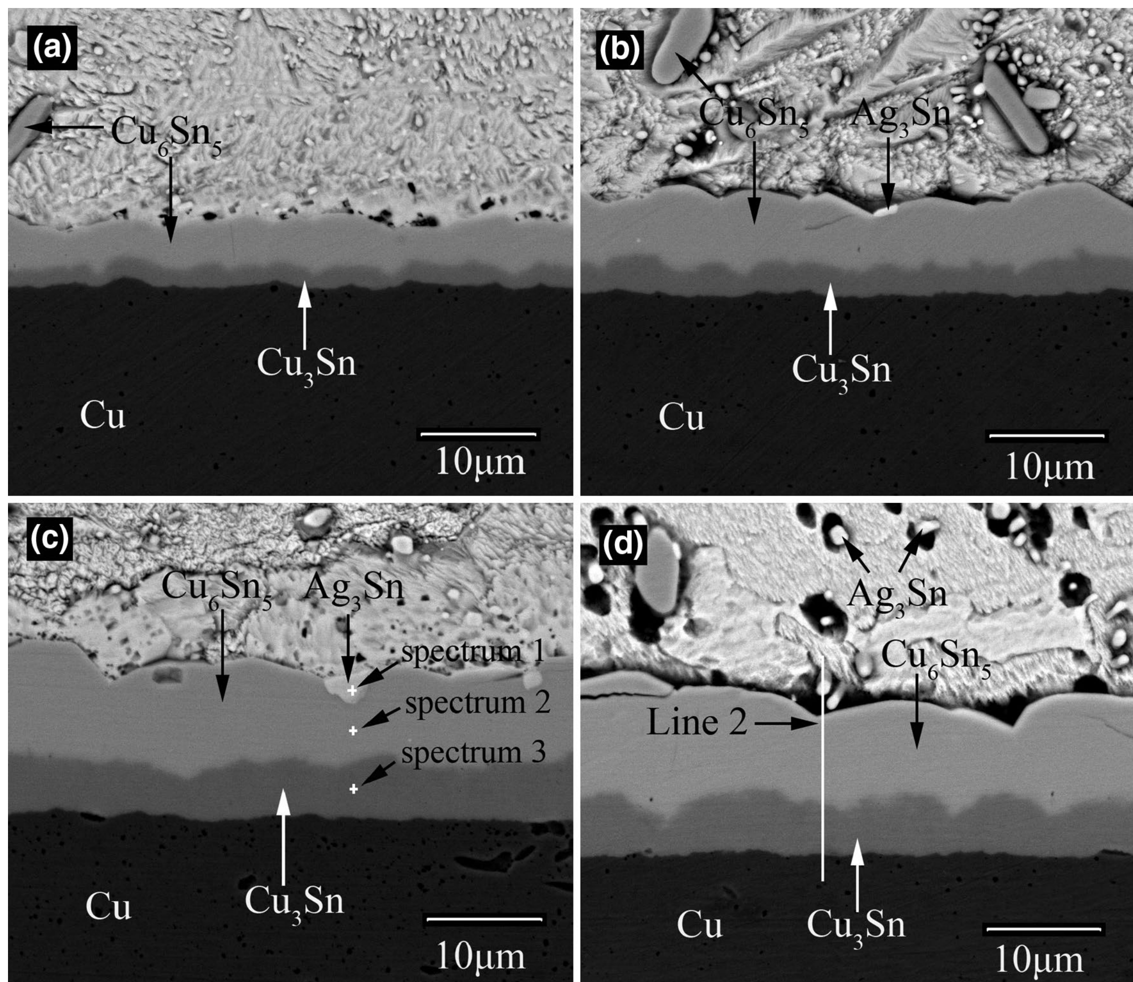

Fig. 3 Cross-sectional microstructure of SAC305/Cu solder joints reflowed at 280 °C for 10 min and aged at 180 °C for various time, **a** 24 h; **b** 120 h; **c** 240 h; **d** 360 h

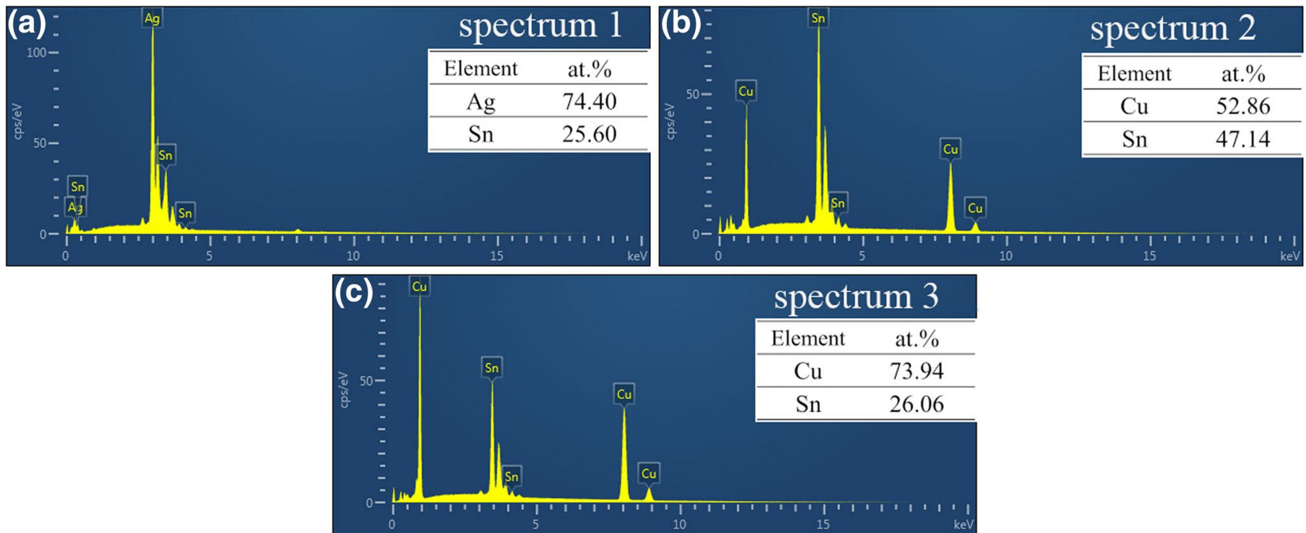

Fig. 4 EDS analysis of IMCs between solder and Cu in Fig. 3c, **a** spectrum 1, **b** spectrum 2, **c** spectrum 3

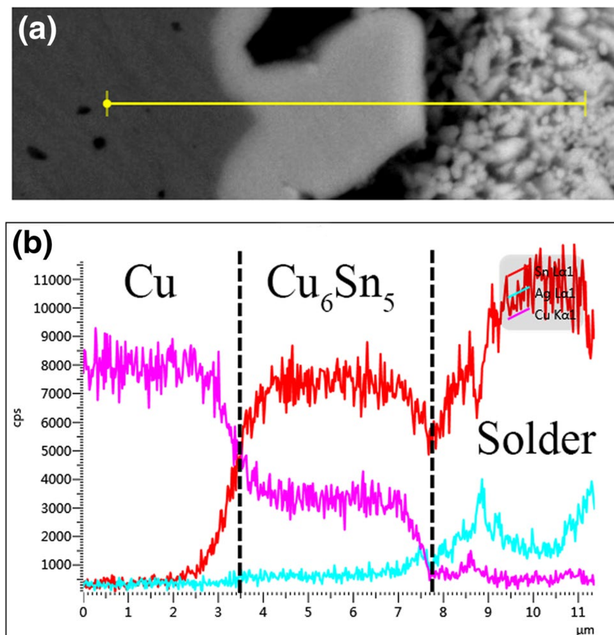

Fig. 5 **a** Close-up BEI micrograph of the line scan 1, **b** elemental counts of line scan 1

different components. The dotted line that isolated different compounds in Fig. 5b can fit perfectly to the boundary of intermetallic compounds in solder/Cu interface as shown in Fig. 5a. From Fig. 5, it can be clearly confirms that there is only scallop-like Cu_6Sn_5 IMC formation after reflowing at 280 °C for 10 min.

Based on the state of identical aging time, microstructure of interfacial IMC in Fig. 2b, Fig. 3a and Fig. 6a were compared. It could be concluded that Cu_3Sn IMC formed in solid-state aging and the higher aging temperature could promote the formation of Cu_3Sn. Besides, the transformation of microstructure and the formation of IMCs at SAC305/Cu interfaces under constant aging temperature were compared also. Figure 2b–e show the cross-sectional BEI micrographs of IMC layer for the interface between Sn3.5Ag0.5Cu solder and Cu substrate aged at 120 °C for 24, 120, 240, 360 h, respectively. It is obviously seen that the IMC thickness is greater with increasing aging time, and the thin Cu_3Sn layer which also be thicker with increasing aging time appeared between Cu_6Sn_5 layer and Cu substrate. With increasing aging time, a large number of bulky Cu_6Sn_5 compounds inlaid in solder and Ag_3Sn particles adhered Cu_6Sn_5 phase emerged at solder joints, as shown in Fig. 2d. Comparing as-aged with as-reflowed samples, the Cu_6Sn_5 compounds became greater and thicker both in solder and interface.

The formation of Cu_3Sn is affected by solid-state reaction, given as Eq. (2):

$$Cu_6Sn_5 + 9\,Cu \rightarrow 5Cu_3Sn \tag{2}$$

It can be deduced that the substantial Cu atoms can diffuse toward to Cu_6Sn_5 to form Cu_3Sn phase during solid-state reaction with long-term aging and high aging temperature, which will represent later. Both long-term aging and high aging temperature can lead Cu atoms to diffuse from substrate toward to solder/Cu interface more quickly. When constant Cu atoms form Cu substrate participated into reaction with the original Cu_6Sn_5 phase to form Cu_3Sn phase, the thickness of Cu_3Sn IMC can be observed with increasing aging time.

Figure 3a–d show the cross-sectional BEI microstructure of SAC305/Cu solder joints reflowed at 280 °C for 10 min and aged at 180 °C for 24, 120, 240 and 360 h, respectively.

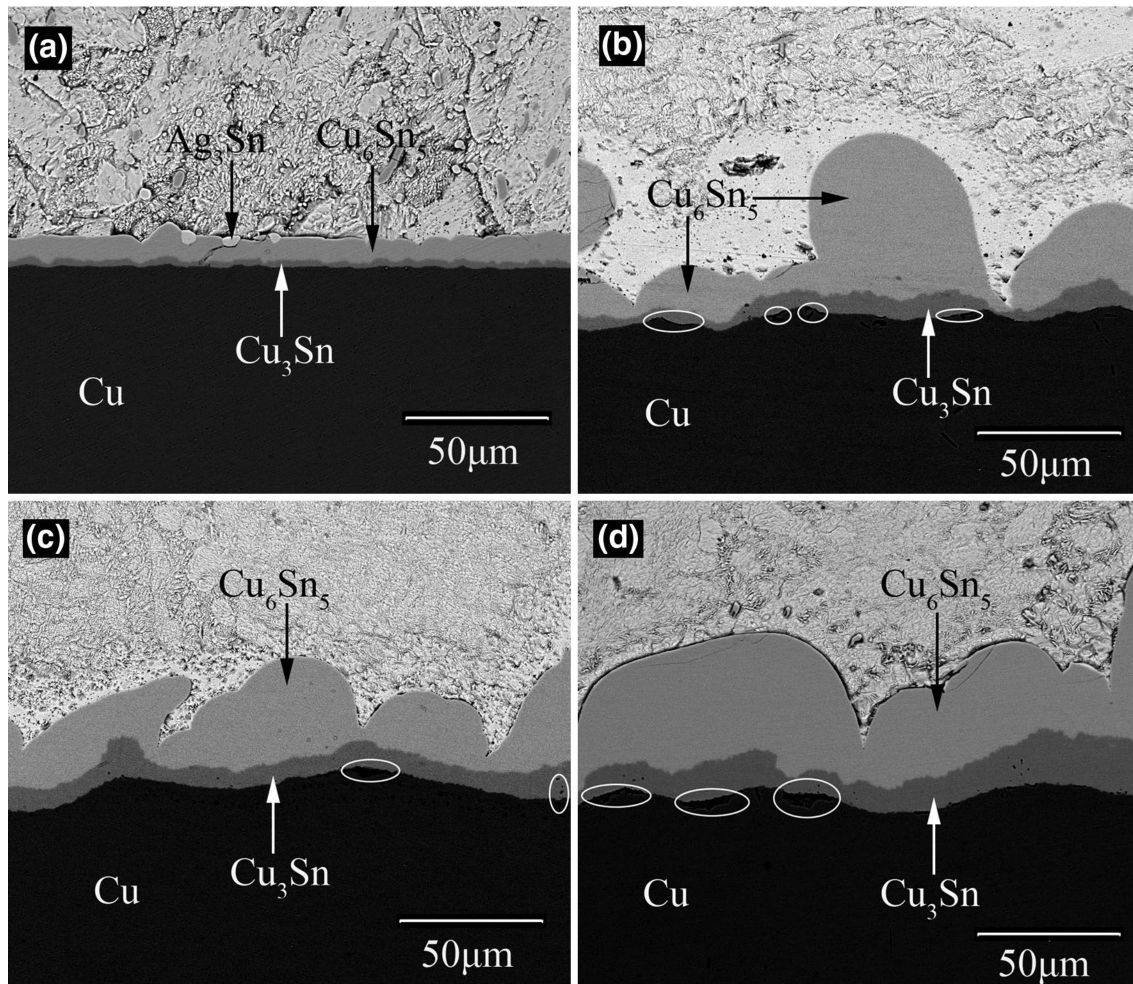

Fig. 6 Cross-sectional microstructure of SAC305/Cu solder joints reflowed at 280 °C for 10 min and aged at 200 °C for various time, **a** 24 h; **b** 120 h; **c** 240 h; **d** 360 h

Under this intermediate temperature, the microstructure of IMC at interface is very different with low-temperature (120 °C) during aging process. As seen from Fig. 3, an even bi-layer of Cu_6Sn_5 phase adjacent to the solder and Cu_3Sn phase adjacent to the Cu substrate were observed in all samples. As shown in Fig. 3a, there were rod-like Cu_6Sn_5 in solder but barely Ag_3Sn particles emerged. After 120 h aged, Ag_3Sn particles can be detected at interface of SAC305/Cu, as shown in Fig. 3b. With increasing aging time, Ag_3Sn particles became greater and accumulated in bulk solder as shown in Fig. 3c, d. In order to further understand the formation of compounds at SAC305/Cu interface after long-time aging, the elemental line scan was applied. The position of line scan 2 was marked by white line as shown in Fig. 3d and the results of elemental line scan were listed in Fig. 7. Figure 7a shows the close-up of the line scan 2 in Fig. 3d. Two intermetallic compound layers with different gray level were observed, and the components were Cu_3Sn and Cu_6Sn_5 which were confirmed by the elemental line scan as shown in Fig. 7b. Comparing Fig. 7a with Fig. 7b, the graininess Ag_3Sn adjacent to interface between solder and Cu_6Sn_5 layer were identified.

To further reveal the distribution of elements at interface of joints after long-time aged, Figs. 2e and 3d with longest aging duration were chosen to show the situations by EDS mapping analysis. Figure 8a, b show the distribution of elements at SAC305/Cu interface after aging for 360 h. Sn mainly consisted in solder with brighter color and partly in IMC layer with darker color. The distribution of Cu element presented similar feature that partly Cu were observed in IMC layer with darker color. Besides, a nubby region which includes Cu element in solder indicated that Cu element in SAC305 solder aggregated and formed compounds after reflowing and aging. Furthermore, Fig. 8b shows difference at Ag element distribution. It clearly seen that Ag aggregated in solder and formed small particles.

Figure 6a–d show that the Cross-sectional BEI microstructure of SAC305/Cu solder joints reflowed at 280 °C for

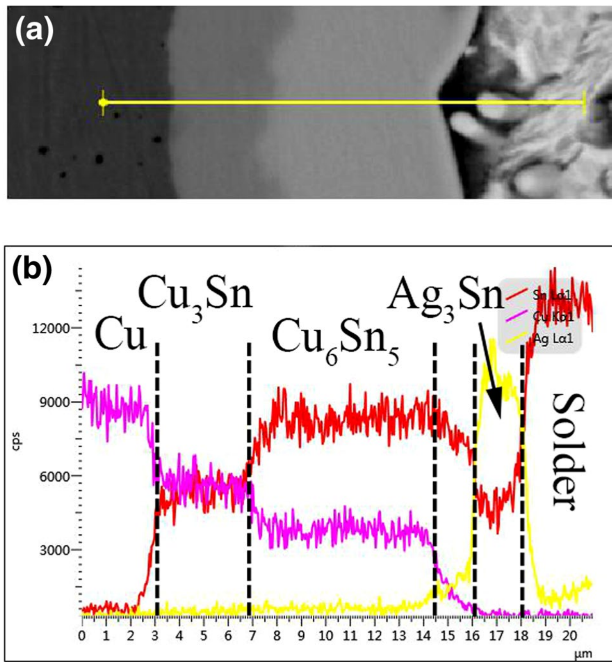

Fig. 7 **a** Close-up BEI micrograph of the line scan 2, **b** elemental counts of line scan 2

10 min and aged at 200 °C for 24; 120; 240; 360 h, respectively. As shown in Fig. 6a, a duplex layer of even Cu_6Sn_5 and intermittent Cu_3Sn IMCs were observed, and Ag_3Sn particles aggregated on the surface of Cu_6Sn_5 layer were detected also. With increasing isotherm aging time, three obvious appearance be observed and list as follow. (1) The thickness of IMCs layer (including both Cu_6Sn_5 and Cu_3Sn) greatly increases under high temperature (200 °C) aging. (2) After aging for 120 h, an uniform IMC layer and planar Cu substrate became extremely uneven and formed raised oval peak. The supply of Cu was relatively abundant for the large solder joints. The morphology of raised oval peak originated from the accumulation of an amount of Cu atom which comes from solder on Cu_6Sn_5 layer surface. The essence of accumulation is that the Cu atoms in solder nucleated by heterogeneous nucleation on surface of existing Cu_6Sn_5 layer. Accordingly, this procedure dominated the morphology of Cu_6Sn_5 layer under high temperature solid-state aging process. (3) A large number of Kirkendall voids which mainly emerged at interface of Cu_3Sn and Cu substrate after long-term solid-state reaction, as indicated with the white circles in Fig. 6b–d. It is well known that the presence of Kirkendall voids will obviously deteriorate the mechanical and impact strength of solder joints. The formation of Kirkendall voids came from vacancies which generated in Cu/Cu_3Sn layer after the Cu atoms have left Cu substrate and diffuse towards the solder. The vacancies coalesce into voids as increasing aging time. This kind vacancy generation in Cu results from unbalanced inter-diffusion of Cu and Sn atoms.

On the whole, three different IMCs patterns corresponding to three temperatures (120, 180 and 200 °C) at solid-state

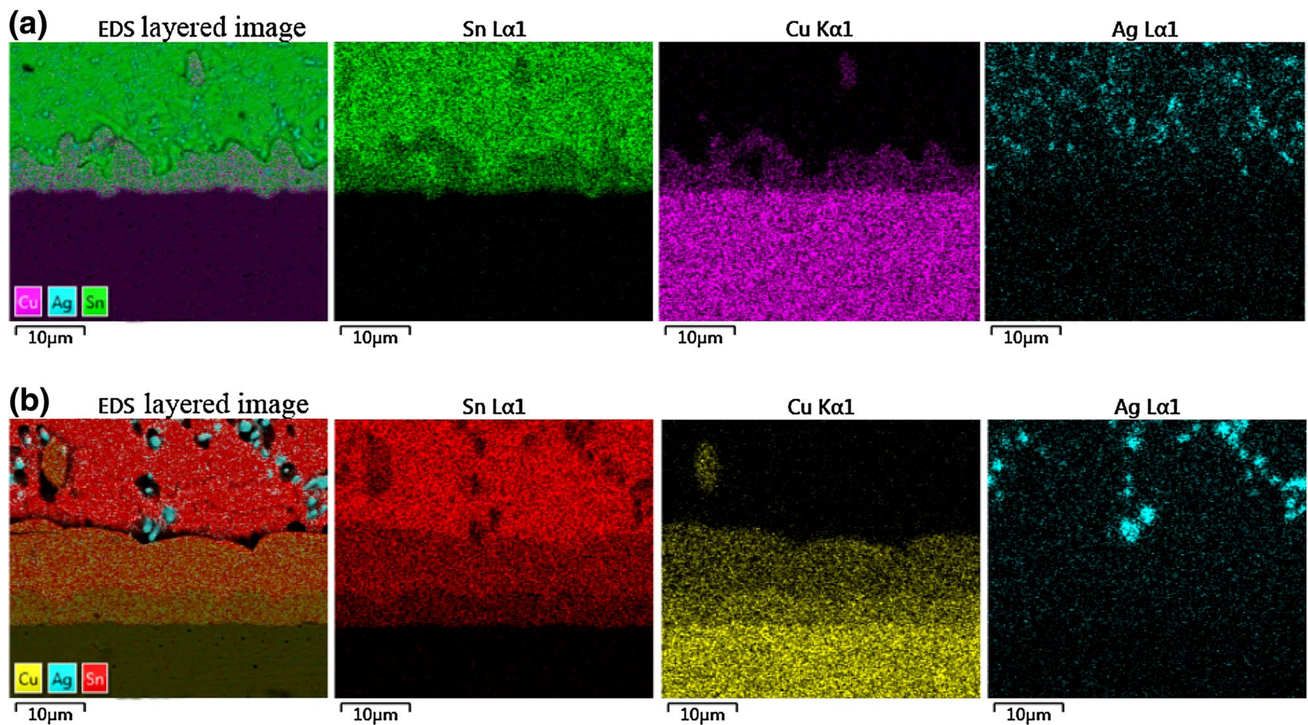

Fig. 8 EDS mapping analysis of SAC305/Cu interface after aging for 360h: **a** at 120 °C; **b** at 180 °C

reaction were observed. After reflowing, only scallop Cu_6Sn_5 formed at solder/Cu interface, as shown in Fig. 2a. When the samples were aged at low temperature, the pattern of IMCs changed slowly and tended to planar, as shown in Fig. 2b–e. With intermediate aging temperature, the thickness of planer IMCs increasing with aging time increases, as shown in Fig. 3. When the samples were subjected to high aging temperature, the planar-like interfacial Cu_6Sn_5 and Cu_3Sn IMCs would transform into wave-like, as shown in Fig. 6. From above phenomenons that various microstructure formed at different aging conditions between SAC305/Cu interfaces, it can draw a conclusion that solid-state aging temperature extremely affect the IMCs microstructure and correspond to different pattern.

Figures 9, 10 and 11 show the top surface morphologies of Cu_6Sn_5 grains formed at the SAC305/Cu interfaces which reflowed at 280 °C for 10 min and aged at 120, 180, 200 °C, respectively. For aging at low and intermediary temperature solder joints, the morphology of Cu_6Sn_5 gradually changed from round shape into polyhedron shape and the IMC size increases with the increasing aging time, which is in agreement with the result of corresponding cross-section (Figs. 2, 3). For the high temperature solder joints, the surface after aged didn't become even and the grains shape turned into large round-cobble, which is also in agreement with the microstructure of cross-section (Fig. 6). According to Kim's research [21], two kinetic processes take effect in growth of Cu_6Sn_5 grains. One is ripening which primary occurred at aging process and another is interfacial reactions. Coalescence is due to the diffusional interaction in which two or more adjacent grains exhibited matching crystal structures and merged together as one, as shown as the marked circles in Fig. 10b. This process will lead to grains volume bigger and amount lesser. Moreover, some cobble-like particles were observed on the Cu_6Sn_5 grains surface, which were confirmed to be Ag_3Sn phase. It is obviously to seen that grains size increases with increasing aging time.

3.2 Growth behavior of Cu–Sn IMCs

The thicknesses of interfacial IMCs layer of all aged SAC305/Cu couples were listed in Table 1. The growth kinetic parameters of an IMC layer can be determined by plotting its measured thickness as a function of the aging time at a given temperature, such as given in Fig. 12. Figure 12a–c represent the IMC layer thickness of aged SAC305/Cu couples which were soldered at 280 °C for 10 min and aged at 120, 180 and 200 °C for various time, respectively. In this study, the Cu_6Sn_5 phase and the Cu_3Sn phase all follow a linear relationship with the square root of the aging time. Accordingly, the growth of IMC during aging process is controlled by the diffusion mechanism. Generally, the relationship between IMC layer thickness and aging duration can be expressed as the following equation [22–24]:

$$L_t = L_0 + kt^{1/2} \tag{3}$$

where L_t is the average thickness of the IMC layer at aging time t, L_0 is the initial thickness before aging, k is the growth rate constant, which is strongly related to the diffusion coefficient of atomic elements of the IMCs, and can be obtained from the linear regression line in this figure. Using this relation, the value of k related to total IMC layer at 120, 180 and 200 °C for SAC305/Cu couples soldered at 280 °C for 10 min was found to be 0.094, 0.534 and 2.442 μm/h$^{1/2}$ (equal to 2.45×10^{-18}, 7.92×10^{-17} and 1.656×10^{-15} m^2/s), respectively, as shown in Fig. 12 and listed in Table 1. In the case of low temperature aging (120 °C), the values of k related to the Cu_6Sn_5 and Cu_3Sn IMC layer are 0.0532 and 0.0441 μm/h$^{1/2}$ (equal to 7.86×10^{-19}, 5.4×10^{-19}m^2/s). When in the case of intermediate temperature aging (180 °C), the values of k related to the Cu_6Sn_5 and Cu_3Sn IMC layer are 0.289 and 0.265 μm/h$^{1/2}$ (equal to 2.32×10^{-17} and 1.95×10^{-17} m^2/s). While in the case of high temperature aging (200 °C), the values of k related to the Cu_6Sn_5 and Cu_3Sn IMC layer are 1.843 and 0.611 μm/h$^{1/2}$ (equal to 9.435×10^{-16} and 1.037×10^{-16} m^2/s). The present results are similar to the previous results for Sn/Cu couples, i.e. 9.25×10^{-17} m^2/s at 150 °C [25].

It is clearly seen that the growth rate of IMC layers is increasing with increasing aging temperature. In this study, the growth rate of Cu_6Sn_5 layer is higher than Cu_3Sn layer for all soldered couples. This phenomenon is contrary to the results that the growth rate of Cu_3Sn layer is higher than Cu_6Sn_5 layer was pointed by Hu [25]. In previous study, the Cu substrate was dipping with pure Sn and aging at 150 °C. Consequently, the solder of pure Sn doesn't contain Cu atoms which differs from SAC305 solder applied in this study. The Cu and Sn formed Cu_6Sn_5 during soldering and aging, in those process, the Cu atoms come from Cu substrate and SAC305 solder. During aging process, the interfacial Cu_6Sn_5 converted to Cu_3Sn by reacting with Cu atoms which come from Cu substrate. However, the growth rate of Cu_6Sn_5 layer is higher than that of Cu_3Sn layer during aging process. It can draw that the reaction of Cu_6Sn_5 formation is faster than that of Cu_3Sn formation converted from Cu_6Sn_5. According to Ming Yang's study [26], Ag inhibited the interfacial IMC growth mostly by slowing the diffusion of Cu atoms, and this resulted in a low fraction of Cu_3Sn in the total IMC formed during solid-state aging. In addition, the solder of SAC305 can provide Cu atoms to formed Cu_6Sn_5 during solid-state aging. Accordingly, the two factors result in that the growth rate of Cu_6Sn_5 layer is higher than that of Cu_3Sn layer. In this study, the high aging temperature (200 °C) approached the solder melting point (217 °C)

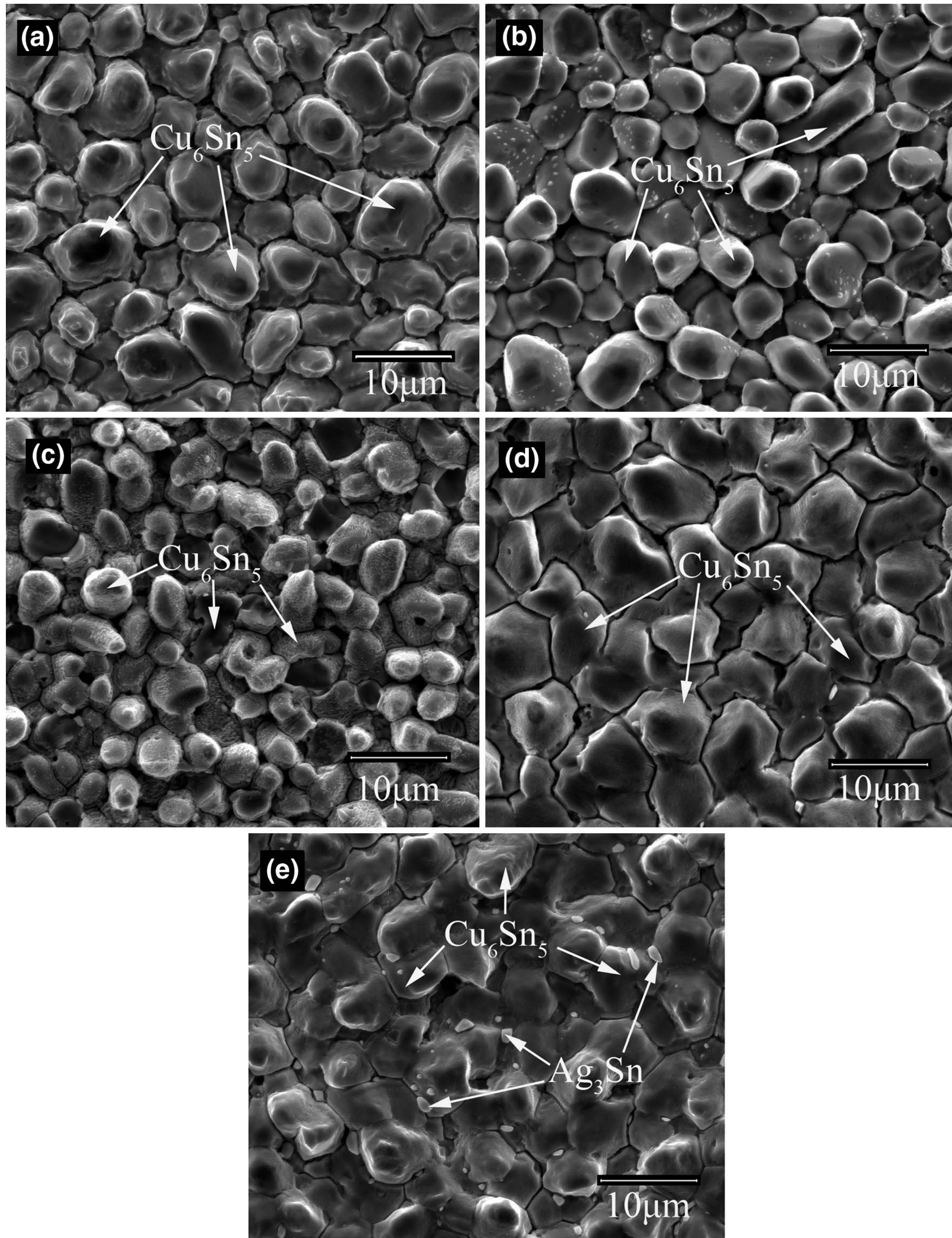

Fig. 9 The morphology of SAC305/Cu interfacial Cu_6Sn_5 grains reflowed at 280 °C for 10 min and aged at 120 °C for various time, **a** reflowed only; **b** 24 h; **c** 120 h; **d** 240 h; **e** 360 h

extremely intensify reaction between solder and Cu substrate. As mentioned above, the large volume solder provided infinite Cu atoms at aging process that could promote the growth of Cu_6Sn_5. The growth rate of Cu_3Sn will not exceed the Cu_6Sn_5 as long as numerous Cu atoms remain in solder.

An Arrhenius relationship was used to determine the activation energy for IMCs layer growth:

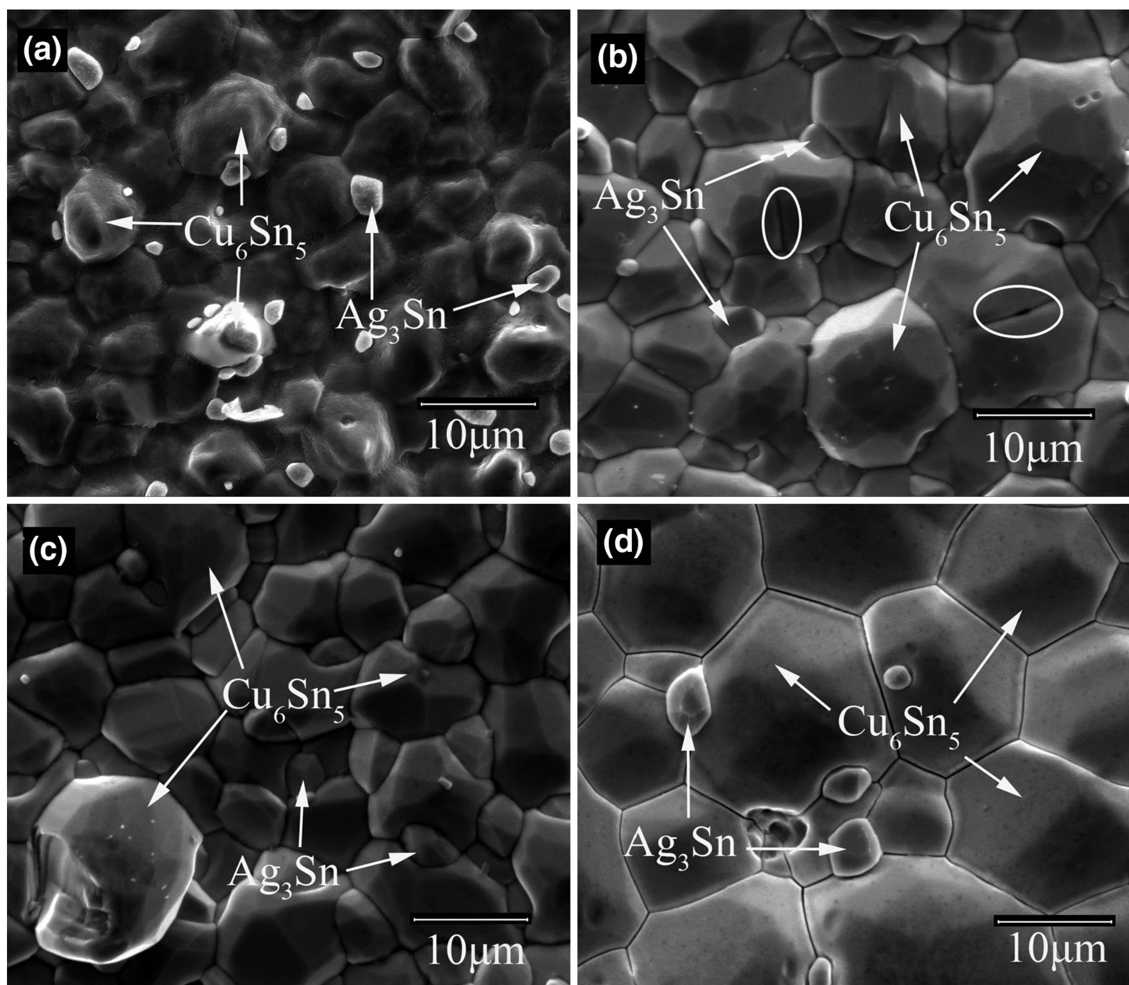

Fig. 10 The morphology of SAC305/Cu interfacial Cu_6Sn_5 grains reflowed at 280 °C for 10 min and aged at 180 °C for various time, **a** 24 h; **b** 120 h; **c** 240 h; **d** 360 h

$$D = D_0 \exp\left(\frac{-Q}{RT}\right) \tag{4}$$

where D is the diffusion coefficient (square of growth rate constant), D_0 is the temperature-independent prefactor, Q is the activation energy, R is the universal gas constant (8.314 J/mol K), and the T the aging temperature (absolute units). Figure 13 shows the Arrhenius plot for the growth of the total Cu–Sn ($Cu_6Sn_5+Cu_3Sn$), Cu_6Sn_5 and Cu_3Sn IMC layers. The activation energy and prefactor can be calculated from the slope and the intercept. Accordingly, the activation energies calculated for the growth of the total Cu-Sn, Cu_6Sn_5 and Cu_3Sn intermetallic are 115.2, 122 and 98 kJ/mol, respectively. In addition, the corresponding prefactors (D_0) are 1.146×10^{-6}, 3.41×10^{-6} and 1.559×10^{-9} $m^2\ s^{-1}$ for the total Cu–Sn, Cu_6Sn_5 and Cu_3Sn IMC layers, respectively. The results of activation energies in the present study are close to the value of 96.75, 85.98 and 105.92 kJ/mol for total Cu–Sn, Cu_6Sn_5 and Cu_3Sn IMC layer in SAC305/Cu couples aging at 100–140 °C [20]. And Zhang [20] pointed out the discrepancy of the activation energies are due to the differences in the preparing process of diffusion couple, aging conditions and analytical method.

To figure out the coarsening mechanism, the diameters of Cu_6Sn_5 grains which were subjected to reflow and thermal aging were measured from the top surface morphology. As shown in Figs. 9, 10 and 11, the Cu_6Sn_5 grains increased in diameter and decreased in number with increasing aging time, and the data of mean diameters of Cu_6Sn_5 grains were listed in Table 2. In order to study the relationship between mean diameters of Cu_6Sn_5 grains and aging time, a log–log plot were presented in Fig. 14. Generally, the relationship of mean diameters of Cu_6Sn_5 grains versus the aging time can be expressed by Eq. (5) [27]:

$$d = Ct^n \tag{5}$$

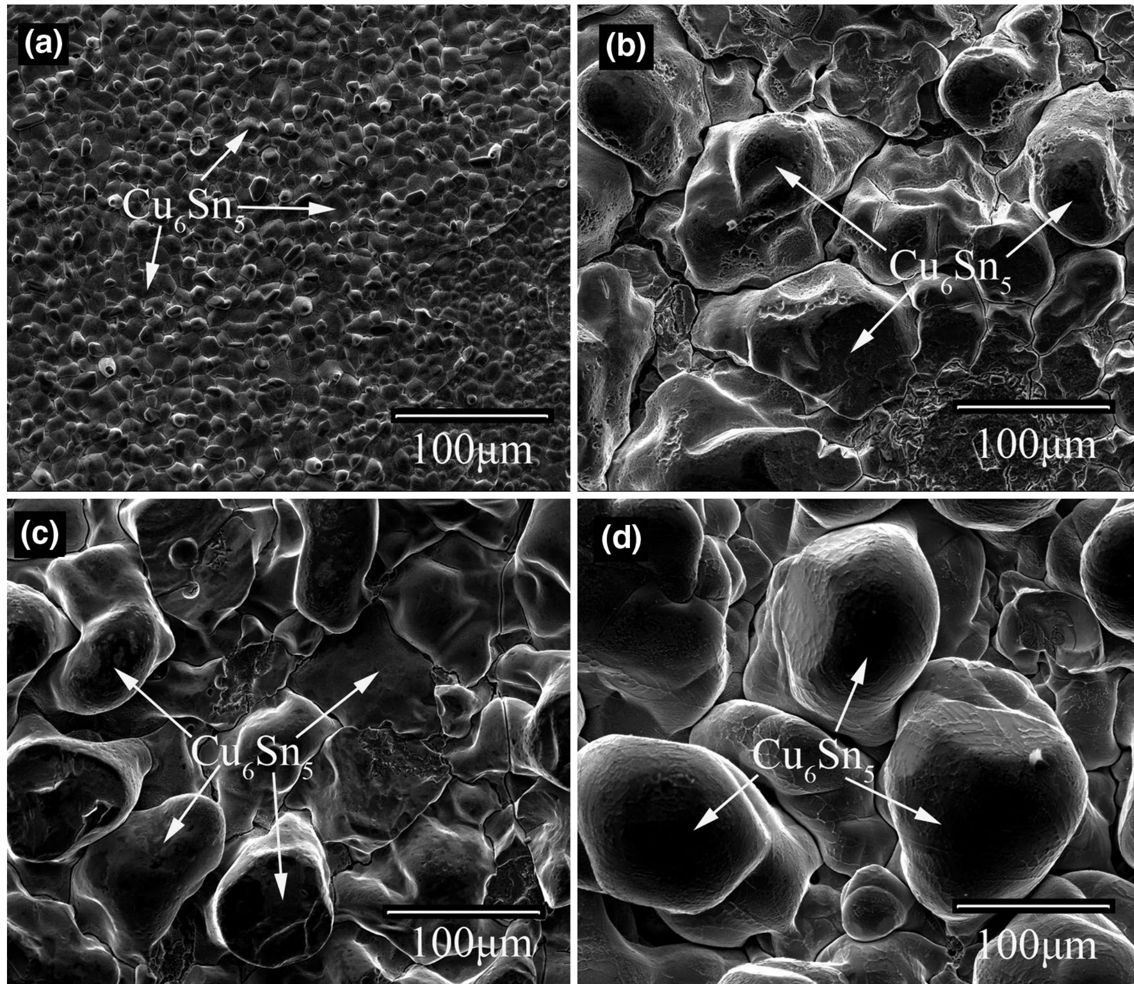

Fig. 11 The morphology of SAC305/Cu interfacial Cu_6Sn_5 grains reflowed at 280 °C for 10 min and aged at 200 °C for various time, **a** 24 h; **b** 120 h; **c** 240 h; **d** 360 h

Table 1 Results of statistical analysis for the mean IMCs thickness of the SAC305/Cu solder joints

Aging time (h)	IMCs thickness (μm)								
	120 °C			180 °C			200 °C		
	Total IMC	Cu_6Sn_5	Cu_3Sn	Total IMC	Cu_6Sn_5	Cu_3Sn	Total IMC	Cu_6Sn_5	Cu_3Sn
0	3.57	3.57	0	3.57	3.57	0	3.57	3.57	0
24	3.6	3.6	0	5.78	4.1	1.68	10.76	8.45	2.31
120	4.326	3.98	0.346	8.57	5.93	2.64	31.65	26	5.65
240	4.783	4.16	0.623	13.28	8.55	4.73	40.39	32.34	8.05
360	6.732	5.97	0.762	13.72	9.2	4.52	47.75	35.58	12.17
Growth rate constant (μm $h^{1/2}$)	0.0974	0.0532	0.0441	0.534	0.289	0.265	2.442	1.843	0.611

where d is the mean diameter of the Cu_6Sn_5 grains, C is the constant, n is the time index and t is the aging time. As seen from Fig. 14, the obtained exponent n is 0.0846 for samples formed at 280 °C aging at 120 °C and 0.184, 0.777 for samples aging at 180 and 200 °C, respectively. which are partly agree with the value of 0.238 for samples formed at 280 °C after 9 days of solid-state aging at 150 °C for Sn37Pb/Cu couples developed by Yang et al. [27]. These results on the exponent are very different to the value of 1/3 developed by the flux-driven ripening (FDR) theory proposed by Tu et al.

Fig. 12 Mean thickness of the IMC layers formed at the SAC305/Cu interface versus the square root of the aging time. **a** aging at 120 °C, **b** aging at 180 °C, **c** aging at 200 ºC

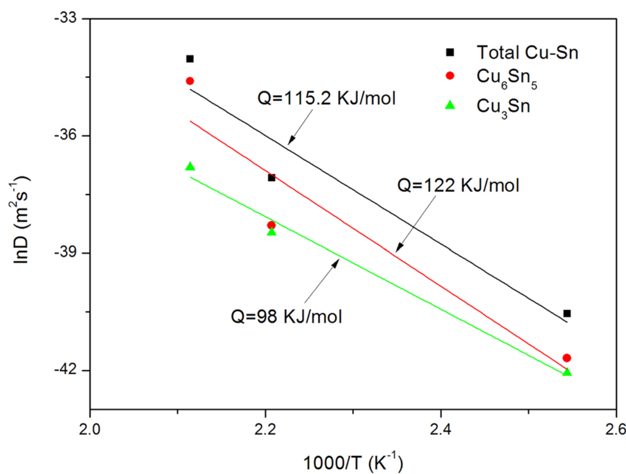

Fig. 13 Arrhenius plot of the IMC layers growth

Table 2 Measured Cu_6Sn_5 grains diameters of aged SAC305/Cu couples

Aging time (h)	Cu_6Sn_5 grain diameter (μm)		
	120 °C	180 °C	200 °C
0	5.05	5.05	5.05
24	5.55	6.64	11.194
120	5.88	8.634	71.07
240	6.5	9.245	82.64
360	7.2	11.83	90.085

[21, 28] for the coarsening mechanism of Cu_6Sn_5 grains formed at a molten solder/solid Cu interface. According to FDR model, the Cu_6Sn_5 grains are assumed to be hemispherical and grow at the expense of their nearest neighbors, which were mentioned at Fig. 10b. However, below 180 °C solid-state aging temperature, the IMC layer become planar

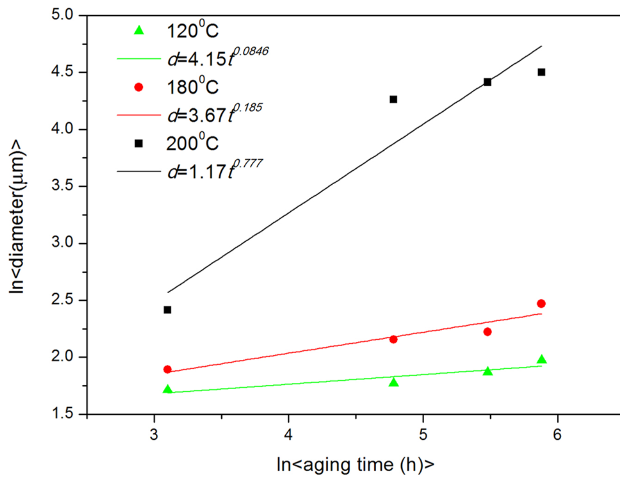

Fig. 14 Average grain diameter of Cu_6Sn_5 of SAC305/Cu solder joints after solid aging for various hours

and the hemispherical grains in liquid-state soldering converted into orthohexagonal grains, as shown in Fig. 10d, when the aging temperature reach 200 °C, the Cu_6Sn_5 grains presented hemispherical as shown in Fig. 11d. In this study, the greatest difference is that the SAC305 solder applied in solder joints contain 0.5 wt% Cu which can extremely affect the IMC morphology and growth rate during high temperature solid-state aging. The solder volume effect that the infinite Cu atoms precipitated on surface of Cu_6Sn_5 to form an uneven interface have been observed in Fig. 6. Therefore, the value of time index (*n)* is different with previous study which applied solder contains barely Cu atoms.

4 Conclusion

The interfacial reaction and growth kinetics of interfacial IMCs layer of SAC305/Cu solder joints during aging at different temperatures were investigated, and the results can be summarized as follows.

1. Only scallop-like Cu_6Sn_5 IMC phase could be found in the interfacial layer after soldering, while Cu_3Sn appeared after aging treatment. The initial scallop-like IMC transformed to a more planar type at low and intermediate aging temperature, but turned to hump at high aging temperature. It can be explained that the numerous Cu atoms from the bulk solder accumulated on the surface of interfacial IMC layer and nucleated by heterogeneous nucleation on formed Cu_6Sn_5 IMC with high aging temperature, which resulted in the faster growth rate of the protruded IMC than that of the planar IMC, therefore, the hump interfacial IMC layer was observed. The Kirkendall voids formed in the neighborhood of the Cu_3Sn/Cu interface and aggregated into continuous regions to form micro-voids.
2. The thickness of total IMC, Cu_6Sn_5 and Cu_3Sn increased linearly with square root of aging time, and the diffusion coefficient increased with increasing aging temperature. The IMC thickness is related to the aging time by $L_t = L + kt^{1/2}$. This equation reveals that a diffusion-controlled mechanism occurrs during aging. The mean diameters of IMC grains were found to increase with increasing aging time, also. Moreover, the relationship can be given as $d = Ct^n$. Due to the volume effect of solder, the growth rate of Cu_6Sn_5 IMC is higher than Cu_3Sn IMC.
3. The activation energies of the total Cu-Sn, Cu_6Sn_5 and Cu_3Sn intermetallic were obtained by plotting the diffusion constants (*D*) as a function of the aging temperature (1/*T*), and were 115.2, 122 and 98 kJ/mol, respectively.

Acknowledgements This work was supported by the Nature Science Foundation of China (Nos. 51465039, 51665038, 51765040) and Nature Science Foundation of Jiangxi Province (20161BAB206122).

References

1. T.L. Yang, J.Y. Wu, C.C. Li, S. Yang, C.R. Kao, Low temperature bonding for high temperature applications by using SnBi solders. J. Alloys Compd. **647**(25), 681–685 (2015)
2. C. Key Chung, Y.J. Chen, C.C. Li, C.R. Kao, The critical oxide thickness for Pb-free reflow soldering on Cu substrate. Thin Solid Films **520**(16), 5346–5352 (2012)
3. Y.W. Wang, Y.W. Lin, C.R. Kao, Kirkendall voids formation in the reaction between Ni-doped SnAg lead-free solders and different Cu substrates. Microelectron. Reliab. **49**(3), 248–252 (2009)
4. M.Y. Tsai, S.C. Yang, Y.W. Wang, C.R. Kao, Grain growth sequence of CuSn in the Cu/Sn and Cu/Sn–Zn systems. J. Alloys Compd. **494**(1), 123–127 (2010)
5. Y.W. Wang, Y.W. Lin, C.T. Tu, C.R. Kao, Effects of minor Fe, Co, and Ni additions on the reaction between SnAgCu solder and Cu. J. Alloys Compd. **478**(1), 121–127 (2009)
6. W.C. Luo, C.E. Ho, J.Y. Tsai, Y.L. Lin, C.R. Kao, Solid-state reactions between Ni and Sn–Ag–Cu solders with different Cu concentrations. Mater. Sci. Eng. **396**(1), 385–391 (2005)
7. S.C. Yang, C.C. Chang, M.H. Tsai, C.R. Kao, Effect of Cu concentration, solder volume, and temperature on the reaction between SnAgCu solders and Ni. J. Alloys Compd. **499**(2), 149–153 (2010)
8. H.W. Yang, J.Y. Wu, Z.X. Zhu, C.R. Kao, Effects of surface diffusion and reaction-induced volume shrinkage on morphological evolutions of micro joints. Mater. Chem. Phys. **191**, 13–19 (2017)
9. Y.W. Wang, Y.W. Lin, C.R. Kao, Inhibiting the formation of microvoids in CuSn by additions of Cu to solders. J. Alloys Compd. **493**(1), 233–239 (2010)
10. F. Wang, L. Zhou, X. Wang et al., Microstructural evolution and joint strength of Sn–58Bi/Cu joints through minor Zn alloying substrate during isothermal aging. J. Alloys Compd. **688**, 639–648 (2016)

11. X. Hu, T. Xu, L.M. Keer et al., Microstructure evolution and shear fracture behavior of aged Sn3Ag0.5Cu/Cu solder joints. Mater. Sci. Eng. A **673**, 167–177 (2016)
12. L. Zhang, L. Sun, Y.H. Guo, Microstructures and properties of Sn58Bi, Sn35Bi0.3Ag, Sn35Bi1.0Ag solder and solder joints. J. Mater. Sci. **26**(10), 1–6 (2015)
13. L. Yang, Y. Zhang, J. Dai et al., Microstructure, interfacial IMC and mechanical properties of Sn–0.7Cu-x Al (x = 0–0.075) lead-free solder alloy. Mater. Des. **67**, 209–216 (2015)
14. L.P. Lehman, S.N. Athavale, T.Z. Fullem et al., Growth of Sn and intermetallic compounds in Sn–Ag–Cu solder. J. Electron. Mater. **33**(12), 1429–1439 (2004)
15. H. Nishikawa, N. Iwata, Formation and growth of intermetallic compound layers at the interface during laser soldering using Sn–Ag Cu solder on a Cu Pad. J. Mater. Process. Technol. **215**(215), 6–11 (2015)
16. Y. Huang, Z. Xiu, G. Wu et al., Improving shear strength of Sn–3.0Ag–0.5Cu/Cu joints and suppressing intermetallic compounds layer growth by adding graphene nanosheets. Mater. Lett. **169**, 262–264 (2016)
17. C. Yang, F. Le, SWR Lee, Experimental investigation of the failure mechanism of Cu–Sn intermetallic compounds in SAC solder joints. Microelectron. Reliab. **62**, 130–140 (2016)
18. AiTingTan,AiWen Tan, Farazila Yusof, Evolution of microstructure and mechanical properties of Cu/SAC305/Cu solder joints under the influence of low ultrasonic power. J. Alloys Compd. **705**, 188–197 (2017)
19. D.Q. Yu, C.M.L. Wu, C.M.T. Law, L. Wang, J.K.L. Lai, Intermetallic compounds growth between Sn–3.5Ag lead-free solder and Cu substrate by dipping method. J. Alloys Compd. **392**(1), 192–199 (2005)
20. L. Zhang, X.Y. Fan, C.W. He et al., Intermetallic compound layer growth between SnAgCu solder and Cu substrate in electronic packaging. J. Mater. Sci. **24**(9), 3249–3254 (2013)
21. H.K. Kim, K.N. Tu, Kinetic analysis of the soldering reaction between eutectic SnPb alloy and Cu accompanied by ripening. Phys. Rev. B, Condens. Matter **53**(23), 16027–16033 (1996)
22. X. Hu, Y. Li, Z. Min, Interfacial reaction and IMC growth between Bi-containing Sn0.7Cu solders and Cu substrate during soldering and aging. J. Alloys Compd. **582**, 341–347 (2014)
23. X. Hu, Y. Li, Z. Min, Interfacial reaction and growth behavior of IMCs layer between Sn–58Bi solders and a Cu substrate. J. Mater. Sci. **24**(6), 2027–2034 (2013)
24. J. Shen, M. Zhao, P. He et al., Growth behaviors of intermetallic compounds at Sn–3Ag–0.5Cu/Cu interface during isothermal and non-isothermal aging. J. Alloys Compd. **574**(10), 451–458 (2013)
25. X. Hu, Z. Ke, Growth behavior of interfacial Cu–Sn intermetallic compounds of Sn/Cu reaction couples during dip soldering and aging. J. Mater. Sci. **25**(2), 936–945 (2014)
26. M. Yang, Y.H. Ko, J. Bang, T.S. Kim, C.W. Lee, M. Li, Effects of Ag addition on solid-state interfacial reactions between Sn–Ag–Cu solder and Cu substrate. Mater. Charact. **124**, 250–259 (2017)
27. M. Yang, M. Li, J. Kim, Texture evolution and its effects on growth of intermetallic compounds formed at eutectic Sn37Pb/Cu interface during solid-state aging. Intermetallics **31**(4), 177–185 (2012)
28. A.M. Gusak, K.N. Tu, Kinetic theory of flux-driven ripening. Phys. Rev. B **66**(11), 115403 (2002)